Effects of rotation on stability of viscous stationary flows on a spherical surface

Ranis N. Ibragimov[1] and Dmitry E. Pelinovsky[2]
[1]*Department of Mathematics, University of Texas at Brownsville, Texas 78520, USA*
[2]*Department of Mathematics, McMaster University, Hamilton, Ontario L8S 4K1, Canada*

(Received 21 April 2010; accepted 19 November 2010; published online 9 December 2010)

We study the incompressible viscous fluid flows within a thin rotating atmospheric shell. The model uses the two-dimensional Navier–Stokes equations on a spherical surface and serves as a simple mathematical description of a general atmospheric circulation caused by the difference in temperature between the equator and the poles. Linearized stability of a particular stationary flow is considered. Under the assumption of no friction and a distribution of temperature dependent only upon latitude, the stationary flow models a zonal distribution of pressure corresponding to atmospheric currents parallel to the circles of latitude. We prove analytically that the stationary flow is asymptotically stable in the time evolution of the Navier–Stokes equations. When the spherical surface is truncated between two symmetrical rings near the North and South Poles, the asymptotic stability of the stationary flow is verified numerically. © *2010 American Institute of Physics*.
[doi:10.1063/1.3526687]

I. INTRODUCTION

The large-scale atmospheric dynamics is usually described by moving air masses on a sphere in terms of three-dimensional Navier–Stokes (NS) equations in a thin rotating spherical shell[1–4] or within the theory of shallow water approximation.[5–7] The modeling of such moving air masses plays an important role in understanding the global climate control.[8] The inclusion of the Coriolis force creates a cyclonic rotation around the poles, i.e., west-to-east winds.[9] Namely, as has been indicated in the late 1800s by Herrmann,[10] the temperature difference between the equator and the poles of a sphere gives rise to waves of two kinds.

The first kind consists of waves that advance in the direction of the meridian; the second kind includes waves that advance in the direction of the circles of latitude. The atmospheric pressures and motions resulting from the combination of these two groups of intersecting waves give rise to the cyclonic and anticyclonic phenomena which are nowadays a paramount topic of research in atmospheric modeling. For example, the mechanisms of cyclone formation in the Earth's atmosphere have been recently studied by Belotserkovskii *et al.*[11] with the help of numerical modeling using the complete system of gas-dynamic equations. The authors of Ref. 11 have shown that cyclones can appear in horizontal stratified shear flows of warm and wet air masses with a horizontal direction of gradients of the wind velocity components as a result of small disturbances of pressure which can be produced by Rossby waves. Recent laboratory experiments on cyclone and anticyclone formation in a rotating stratified fluid have been studied by Cenedese and Linden.[12] The importance of understanding the formation of cyclones and their time evolution in the Earth's atmosphere for the creation and distribution of weather systems throughout the world is summarized by Summerhayes and Thorpe.[8]

The dominant feature of the upper-air flow in midlatitudes is strong, westerly currents circling the Earth. These currents include long waves with lengths of several thousand kilometers so that there are only two or three waves around the entire hemisphere. Since westerly winds in the southern hemisphere are an important force contributing to climate modulation,[13,14] understanding of the large-scale atmospheric dynamics is the topic of current extensive research. For example, recent studies by Shindell and Schmidt[15] suggest that global warming has increased the temperature difference between the southern, mid-, and high-latitudes and loss of Antarctic ozone have contributed to this increase.

In terms of mathematical analysis of the NS equations in a thin spherical shell, the convergence of the longitudinal velocity averaged in the radial direction across the shell to the strong solution to the two-dimensional NS equations on a sphere as the thickness of the shell converges to zero has been rigorously proved by Temam and Ziane.[16] The treatment of geometric singularities in spherical coordinates has for many years been a difficulty in the development of numerical simulations for oceanic and atmospheric flows around the Earth. In particular, Blinova[1,2] represented solutions in the inviscid case by eigenfunction expansions in spherical harmonics. Vorticity equations were considered by Ben-Yu[17] using the spectral method. In terms of numerical simulations, most of studies use a powerful Jacobi–Davidson "QZ" method[18] to solve the resulting linearized eigenvalue problem (see also Weijer *et al.*[7] for implementation of this method in studying the barotropic Rossby basin modes of the Argentine Basin). This method is based on calculating eigenvalues that are closest to a prespecified target value.

The accuracy of finite-differences approximations for solving differential equations describing fluid flow on the surface of the sphere is discussed by Williamson *et al.*[19] Three of the seven test problems studied in Ref. 19 are closely related to our model. The first test consists of advec-

tion of a compactly supported structure by a specific wind field corresponding to solid body rotation whose axis is not necessarily coincident with that of the Earth's rotation. As such this case deals with only a subset of the shallow water equations, namely, the continuity equation, but concentrates on the scheme's ability to deal with poles of the spherical coordinate system. The second and the third cases present the steady state, nonlinear zonal flow, and represent a global form with the wind corresponding to solid body rotation and a local form where the wind field has a compact support. In both latter cases the spherical coordinate poles are not necessarily coincident with the Earth's rotation axis.

Callaghan and Forbes[20] considered the flow of a thin layer of an incompressible fluid on a rotating sphere to study a linearized theory for small amplitude perturbations about a stationary flow. They extended their result to the numerical solution of the full model in the absence of viscosity, to obtain highly nonlinear large-amplitude progressive-wave solutions in the form of Fourier series. It is shown in Ref. 20 that the formation of localized low pressure systems cut off from the main flow field is an inherent feature of the nonlinear dynamics, once the amplitude forcing reaches a certain critical level.

The problem which forms our main focus of interest here is to study the linearized stability of exact stationary solutions associated with the west-to-east flows in a thin rotating spherical shell. In our previous work,[21] we studied the linearized stability of incompressible viscous fluid flows in a thin spherical shell, using the two-dimensional NS equations on a sphere which ignore the effects of rotation. Here we aim to consider long waves formed in the Earth's atmosphere, which is captured by the rotation of the Earth, with a further goal to extend our analysis to the case when the effects of rotation are incorporated in the modeling equations. In particular, as it has been remarked by Herrmann,[10] under the assumption of no friction and a distribution of temperature dependent only upon latitude, starting from some height, the west-to-east flows always exist in the Earth's atmosphere. The possible modeling scenario when a steady condition of motion can occur in the atmosphere with a constant distribution of temperature has also been discussed in Ref. 10. The experimental results by Cenedese and Linden[12] justify many of the conclusions discussed by Herrmann.[10]

In this work we focus on stability of latitude-dependent stationary exact solutions of the NS equations in a rotating thin spherical shell. The inquiry is motivated by dynamically significant Coriolis forces in atmospheric and oceanographic applications such as a climate variability models and the general atmospheric (or oceanic) circulation model.

The exact solution discussed here is used to describe physically relevant zonal flows. For example, the presence of the Coriolis force creates a cyclonic rotation around the poles, i.e., west-to-east winds. From a mathematical standpoint, the velocity and the pressure terms are unbounded in the neighborhood of the pole. Unbounded terms are common in differential equations posed in spherical coordinates (see e.g., Swarztrauber[22]). Computational experiments[6,7,17,22] provide a credible evidence to support the assertion that singular solutions to the shallow water equations may exist on a stationary sphere. They also suggest that singular solutions are less likely on a rotating sphere. However, the experiments conducted up to the date are not sufficiently extensive to support any credible evidence on the existence or nonexistence of singular solutions to the shallow water equations on a rotating sphere. Even less is known about singular terms used on a spherical surface.

From the practical standpoint, it is useful to note that the fluid particles at the North and South Poles spin around themselves at a rate $\Omega=2\pi$ rad/day, whereas fluid particles in the domain $\theta\in[\theta_0,\pi-\theta_0]$ do not spin around themselves but simply translate provided $\theta_0\in(0,\frac{\pi}{2})$. Owing to the Coriolis effects, the achievable meteorological flows rotating around the poles correspond to the flows that are being translated along the equatorial plane. This translational motion is well captured by the exact solutions for the zonal flows considered in our work.

The paper is organized as follows. Section II gives a mathematical formulation of the problem. Section III sets up the stationary flow and the linearized equations. Section IV is devoted to the analytical proof of spectral stability of the stationary flow. Section V gives the results of numerical approximations of eigenvalues. Section VI concludes the paper with some remarks.

II. WAVES IN A ROTATING SPHERICAL SHELL

Our starting point is the equations of motion for a viscous fluid in the Lamb's form[23]

$$\begin{cases} \dfrac{\partial \mathbf{v}}{\partial t} - \mathbf{v}\times(\nabla\times\mathbf{v}) = -\nabla\left(\dfrac{1}{2}\mathbf{v}\cdot\mathbf{v} + p + W\right) + \nu\Delta\mathbf{v} + 2\mathbf{v}\times\boldsymbol{\Omega}, \\ \nabla\cdot\mathbf{v} = 0, \end{cases} \tag{1}$$

where $\mathbf{v}\in\mathbb{R}^3$ is the velocity vector, p is the pressure, ν is the kinematic viscosity, W is the potential of the gravitational force which includes the Newtonian attraction and the centrifugal force of the rotation of the Earth, and $\boldsymbol{\Omega}$ represents the Coriolis force. We consider the fluid in a thin spherical shell

$$\Pi = \{\mathbf{x} \in \mathbb{R}^3 : r_0 < |\mathbf{x}| < r_0 + \epsilon\},$$

where r_0 is a fixed altitude above the Earth and ϵ is a small parameter for the thickness of the spherical shell. System (1) is supplemented with the homogeneous boundary condition

$$\mathbf{v} \cdot \mathbf{n} = 0, \quad (\nabla \times \mathbf{v}) \times \mathbf{n} = \mathbf{0}, \quad \mathbf{x} \in \partial\Pi,$$

where $\partial\Pi$ is the boundary of the spherical shell Π and $\mathbf{n}$ is the normal vector to the boundary.

We now employ the usual spherical coordinates (r, θ, ϕ) with the velocity vector

$$\mathbf{v} = v_r \mathbf{e}_r + v_\theta \mathbf{e}_\theta + v_\phi \mathbf{e}_\phi,$$

where $(\mathbf{e}_r, \mathbf{e}_\theta, \mathbf{e}_\phi)$ are basic orthonormal vectors in spherical coordinates. We denote θ as the polar (latitude) angle and ϕ as the azimuthal (longitude) angle, so that v_θ is associated with the velocity component along the meridian (which is positive when the velocity is directed to the south) and v_ϕ is associated with the velocity component along the circle of the latitude (which is positive when it is directed toward the east).

As $\varepsilon \to 0$, the three-dimensional NS Eq. (1) can be reduced to the two-dimensional equations on the sphere

$$S = \{(\theta, \phi), \ 0 \le \theta \le \pi, \ 0 \le \phi < 2\pi\}, \tag{2}$$

where $0 < \varepsilon < 1$ is a nondimensional small parameter. This reduction is based on the result of theorem B in Temam and Ziane,[16] which states that provided the initial data are smooth enough, the strong global solution $\mathbf{v}(r, \theta, \phi, t)$ of the three-dimensional NS equations converges as $\varepsilon \to 0$ to the strong global solution $\mathbf{u}(\theta, \phi, t)$ of the two-dimensional NS equations on the sphere, where

$$\mathbf{u}(\theta, \phi, t) = \lim_{\varepsilon \to 0} \frac{1}{\varepsilon r_0} \int_{r_0}^{r_0 + \varepsilon r_0} r\mathbf{v}(r, \theta, \phi, t) dr = (0, u_\theta, u_\phi).$$

The vector $\mathbf{u}(\theta, \phi, t)$ can be interpreted as the *average velocity* with respect to r.

It is useful to recast the model in nondimensional form by taking c_0 as the unit of velocity, r_0 as the unit of length, and defining the Reynolds number R_e and the Rossby number R_0 as follows

$$R_e = \frac{c_0 r_0}{\nu}, \quad R_0 = \frac{c_0}{2\Omega r_0}, \tag{3}$$

where $\Omega = 2\pi$ rad/day $\approx 0.73 \times 10^{-4}$ s^{-1} is the rate of the Earth's rotation. After the averaging procedure, the two-dimensional NS equations in spherical angles are written as follows

$$\frac{\partial u_\theta}{\partial t} + u_\theta \frac{\partial u_\theta}{\partial \theta} + \frac{u_\phi}{\sin(\theta)} \frac{\partial u_\theta}{\partial \phi} - u_\phi^2 \cot(\theta) - \frac{u_\phi \cos(\theta)}{R_0} = -\frac{\partial p}{\partial \theta} + \frac{1}{R_e} \left\{ \Delta_S u_\theta - \frac{1}{\sin^2(\theta)} \left[u_\theta + 2 \frac{\partial u_\phi}{\partial \phi} \cos(\theta) \right] \right\}, \tag{4}$$

$$\frac{\partial u_\phi}{\partial t} + u_\theta \frac{\partial u_\phi}{\partial \theta} + \frac{u_\phi}{\sin(\theta)} \frac{\partial u_\phi}{\partial \phi} + u_\theta u_\phi \cot(\theta) + \frac{u_\theta \cos(\theta)}{R_0} = -\frac{1}{\sin(\theta)} \frac{\partial p}{\partial \phi} + \frac{1}{R_e} \times \left\{ \Delta_S u_\phi - \frac{1}{\sin^2(\theta)} \left[u_\phi - 2 \frac{\partial u_\theta}{\partial \phi} \cos(\theta) \right] \right\}, \tag{5}$$

$$\frac{\partial}{\partial \theta} [u_\theta \sin(\theta)] + \frac{\partial u_\phi}{\partial \phi} = 0, \tag{6}$$

where

$$\Delta_S = \frac{1}{\sin(\theta)} \left\{ \frac{\partial}{\partial \theta} \left[\sin(\theta) \frac{\partial}{\partial \theta} \right] + \frac{1}{\sin(\theta)} \frac{\partial^2}{\partial \phi^2} \right\} \tag{7}$$

is the Laplace–Beltrami operator in spherical angles.

One can check by direct differentiation that there exists an exact stationary solution to the two-dimensional NS Eqs. (4)–(6) given by

$$u_\theta = 0, \quad u_\phi = \frac{1}{\sin(\theta)}, \qquad p = \int \cot(\theta) \left[\frac{1}{\sin^2(\theta)} + \frac{1}{R_0} \right] d\theta + p_0, \tag{8}$$

where p_0 is an arbitrary constant.

Equations (4)–(6) are written in a noninertial reference frame. Coriolis effects are generated by the pseudoforces, which support the west-to-east flows that are related to jet streams, i.e., zones of fast moving west-to-east winds in the upper atmosphere between the Ferrell and Polar cells. Thus, under the assumption of no friction and a distribution of temperature dependent only upon latitude and altitude, the stationary solution (8) can be associated with a zonal flow directed from the west to east.

III. LINEARIZATION AND NORMAL MODE ANALYSIS

For the purposes of our work, we rewrite the two-dimensional NS Eqs. (4)–(6) on the sphere S in an equivalent form

$$\frac{\partial u_\theta}{\partial t} - \frac{\omega u_\phi}{\sin(\theta)} + \frac{\partial q}{\partial \theta} - \frac{u_\phi \cos(\theta)}{R_0} = \frac{1}{R_e} \left[\Delta_S u_\theta - \frac{2\cos(\theta)}{\sin^2(\theta)} \frac{\partial u_\phi}{\partial \phi} - \frac{u_\theta}{\sin^2(\theta)} \right], \tag{9}$$

$$\frac{\partial u_\phi}{\partial t} + \frac{\omega u_\theta}{\sin^2(\theta)} + \frac{1}{\sin(\theta)} \frac{\partial q}{\partial \phi} + \frac{u_\theta \cos(\theta)}{R_0} = \frac{1}{R_e} \left[\Delta_S u_\phi + \frac{2\cos(\theta)}{\sin^2(\theta)} \frac{\partial u_\theta}{\partial \phi} - \frac{u_\phi}{\sin^2(\theta)} \right], \tag{10}$$

$$\frac{\partial}{\partial \theta} [u_\theta \sin(\theta)] + \frac{\partial u_\phi}{\partial \phi} = 0, \tag{11}$$

where q is a static (stagnation) pressure and ω is the vorticity

$$q = p + \frac{1}{2}(u_\theta^2 + u_\phi^2), \quad \omega = \frac{\partial}{\partial\theta}[u_\phi \sin(\theta)] - \frac{\partial u_\theta}{\partial\phi}. \tag{12}$$

Accordingly, as follows from Eqs. (8) and (12), the exact stationary solution to the two-dimensional NS Eqs. (9)–(11) is given by

$$u_\theta = 0, \quad u_\phi = \frac{1}{\sin(\theta)}, \quad q = \frac{1}{R_0}\int \cot(\theta)d\theta + q_0, \tag{13}$$

where q_0 is an arbitrary constant. We linearize Eqs. (9) and (10) at the basic solution (13). The linear evolution equations are

$$\frac{\partial u_\theta}{\partial t} - \frac{1}{\sin(\theta)}\left[\frac{u_\phi \cos(\theta)}{\sin(\theta)} + \frac{\partial u_\phi}{\partial\theta} - \frac{1}{\sin(\theta)}\frac{\partial u_\theta}{\partial\phi}\right] + \frac{\partial q}{\partial\theta} - \frac{u_\phi \cos(\theta)}{R_0} = \frac{1}{R_e}\left[\Delta_S u_\theta - \frac{2\cos(\theta)}{\sin^2(\theta)}\frac{\partial u_\phi}{\partial\phi} - \frac{u_\theta}{\sin^2(\theta)}\right], \tag{14}$$

$$\frac{\partial u_\phi}{\partial t} + \frac{1}{\sin(\theta)}\frac{\partial q}{\partial\phi} + \frac{u_\theta \cos(\theta)}{R_0} = \frac{1}{R_e}\left[\Delta_S u_\phi - \frac{u_\phi}{\sin^2(\theta)} + \frac{2\cos(\theta)}{\sin^2(\theta)}\frac{\partial u_\theta}{\partial\phi}\right]. \tag{15}$$

In view of the divergence-free condition (11), we perform a normal mode analysis by

$$u_\theta = \frac{ikg(\theta)}{\sin(\theta)}e^{ik\phi}e^{\lambda t/R_e}, \quad u_\phi = -g'(\theta)e^{ik\phi}e^{\lambda t/R_e}, \quad q = Q(\theta)e^{ik\phi}e^{\lambda t/R_e}, \tag{16}$$

where $\lambda \in \mathbb{C}$ is a parameter and $k \in \mathbb{Z}$ is the Fourier wave number. Perturbations with $\lambda_r = \mathrm{Re}(\lambda) > 0$ imply spectral instability of the stationary flow (13). If $\lambda_r < 0$ for all perturbations, the stationary flow is asymptotically stable.

Substituting the eigenmode solutions (16) into the governing Eqs. (14) and (15) and neglecting the quadratic terms of the perturbation yields the following eigenvalue problem:

$$L_k g(\theta) + \frac{\cos(\theta)\sin(\theta)}{R_0}g'(\theta) + \frac{ik\lambda}{R_e}g(\theta) + \sin(\theta)Q'(\theta) = \frac{ikL_k g(\theta)}{R_e}, \tag{17}$$

$$-\frac{ik\cos(\theta)}{R_0\sin(\theta)}g(\theta) + \frac{\lambda}{R_e}g'(\theta) - \frac{ikQ(\theta)}{\sin(\theta)} = \frac{1}{R_e}\frac{d}{d\theta}L_k g(\theta), \tag{18}$$

where L_k is the Sturm–Liouville operator for the associated Legendre functions

$$L_k = \frac{1}{\sin(\theta)}\frac{d}{d\theta}\left[\sin(\theta)\frac{d}{d\theta}\right] - \frac{k^2}{\sin^2(\theta)}. \tag{19}$$

Eliminating Q from Eqs. (17) and (18), we get to the following equation:

$$-ikR_e \sin^2(\theta)\left[L_k + \frac{\sin^2(\theta)}{R_0}\right]g - F = 0, \tag{20}$$

where we denote

$$F = -\sin^4(\theta)g''''(\theta) - 2\cos(\theta)\sin^3(\theta)g'''(\theta) + \sin^2(\theta)\times[2k^2 + 1 + \sin^2(\theta)(1+\lambda)]g''(\theta) - \cos(\theta)\sin(\theta)\times[1 + 2k^2 - \lambda\sin^2(\theta)]g'(\theta) + \{2k^2[1+\cos^2(\theta)] - k^4 - k^2\lambda\sin^2(\theta)\}g(\theta).$$

We next define f by $f = L_k g$. Then, F becomes

$$F = \sin^4(\theta)\left\{\left[\lambda + \frac{k^2}{\sin^2(\theta)}\right]f - \frac{\cos(\theta)}{\sin(\theta)}f'(\theta) - f''(\theta)\right\}.$$

Substituting this expression into Eq. (20), we obtain

$$-ik\sin^2(\theta)\left[L_k + \frac{\sin^2(\theta)}{R_0}\right]g - \frac{1}{R_e}\sin^4(\theta)(\lambda f - L_k f) = 0. \tag{21}$$

As a result, the coupled eigenvalue problem for f and g is written in the form

$$L_k g = f, \quad L_k f - \lambda f = ikR_e\left[\frac{f}{\sin^2(\theta)} + \frac{g}{R_0}\right]. \tag{22}$$

We shall now set up boundary conditions for the eigenvalue problem (22). Since $\theta = 0$ and $\theta = \pi$ are singular end points of the differential Eq. (22), the boundary conditions are obtained from the requirement that components of $\sin(\theta)u_\theta$ and $\sin(\theta)u_\phi$ vanish at the North and South Poles. Using Eq. (16), we obtain

$$\lim_{\theta\to 0} g(\theta) = \lim_{\theta\to\pi} g(\theta) = 0 \tag{23}$$

and

$$\lim_{\theta\to 0} \sin(\theta)g'(\theta) = \lim_{\theta\to\pi} \sin(\theta)g'(\theta) = 0. \tag{24}$$

For a typical atmosphere, we can choose the characteristic velocity and length scale to be $c_0 \sim 10$ m/s, and $r_0 \sim 10^3$ (see also Table I in Ref. 7) so that, according to the definition (3) for the Rossby number R_0, we have

$$\frac{1}{R_0} = \frac{2\Omega r_0}{c_0} \approx 0.0146.$$

A small Rossby number R_0 signifies a system which is strongly affected by Coriolis force, and a large Rossby number R_0 signifies a system in which inertial and centrifugal forces dominate. As is seen from the above computation, our model is related to the second situation of the large Rossby numbers.

A. Comparison with the case of zero rotation

The case of zero rotation ($R_0 = \infty$) gives a system of equations

$$L_k g = f, \quad L_k f - \lambda f = \frac{ikR_e f}{\sin^2(\theta)}, \tag{25}$$

where the equation on f is decoupled.

System (25) is different from system (3.1) in our previous work[21] because the steady-state profile is different from Eq. (13). In Ref. 21, we studied stability of the steady-state flow

$$u_\theta = \frac{1}{\sin(\theta)}, \quad u_\phi = 0, \quad q = q_0,$$

where q_0 is a constant. This steady-state flow exists for the case of zero rotation ($R_0=\infty$) but does not persist if the rotation is included ($R_0<\infty$). For comparison, the eigenvalue problem considered in Ref. 21 takes the form

$$L_k g = f, \quad L_k f + \frac{1}{R_e} f' = \lambda f.$$

If the rotation is included ($R_0<\infty$), then the system of Eq. (22) is

$$L_k g = f, \quad L_k f - \lambda f = \frac{ikR_e}{\sin^2(\theta)} f + \frac{ikR_e}{R_0} g \tag{26}$$

and the equations on f and g are coupled. It follows directly from our previous analysis in Ref. 21 that the steady-state solution (13) is asymptotically stable with respect to symmetry-preserving perturbations ($k=0$) for all possible Reynolds numbers (proposition 8 in Ref. 21). However, for symmetry-breaking perturbations ($k \in \mathbb{N}$), we need to study distribution of eigenvalues in the linearized system (26).

We note that if all functions (u_θ, u_ϕ, q) are independent of ϕ, then there is a reduction $u_\theta=0$ of the two-dimensional NS Eqs. (9)–(11). This reduction allows us to close the system of nonlinear equations at the linear evolution equation

$$\frac{\partial u_\phi}{\partial t} = \frac{1}{R_e}\left[\Delta_S u_\phi - \frac{u_\phi}{\sin^2(\theta)}\right].$$

Substituting

$$u_\theta = \frac{1}{\sin(\theta)} - g'(\theta) e^{\lambda t/R_e}$$

and integrating in θ gives the closed equation $L_0 g = \lambda g$, which replaces system (26) for $k=0$. As mentioned above, the eigenvalue problem $L_0 g = \lambda g$ subject to the boundary conditions (24) has all eigenvalues with $\mathrm{Re}(\lambda)<0$.

IV. EIGENVALUES OF THE LINEARIZED PROBLEM

Let us fix $k \in \mathbb{N}$. We shall separate the case of zero rotation, when the eigenvalues of the linearized system (25) can be computed exactly, and the case of nonzero rotation, when the eigenvalues of the linearized system (26) can only be approximated asymptotically and numerically. In both cases, we show that the steady-state solution is asymptotically stable with respect to linearization because all eigenvalues of the linearized systems have negative real parts.

A. The case of zero rotation

We consider the linearized problem (25) which arises when $R_0=\infty$. Let $z=\cos(\theta)$ and regard f and g as functions of z. The differential operator L_k is written as

$$L_k = \frac{d}{dz}\left[(1-z^2)\frac{d}{dz}\right] - \frac{k^2}{1-z^2} \tag{27}$$

and the boundary conditions (23) and (24) become

$$\lim_{z\to\pm 1} g(z) = \lim_{z\to\pm 1} (1-z^2) g'(z) = 0. \tag{28}$$

For any nonzero $g \in \mathrm{Dom}(L_k) \subset L^2([-1,1])$ and $h \in L^2([-1,1])$, integration by parts yields

$$(L_k g, h) = -\int_{-1}^{1} \left[(1-z^2) g'(z) h'(z) + \frac{k^2}{1-z^2} g(z) h(z)\right] dz, \tag{29}$$

where the boundary conditions (28) have been used. Since the form $(L_k g, h)$ represents a bounded and coercive bilinear functional, by the Lax–Milgram theorem (see e.g., Zeidler[24]), L_k is invertible and there is a unique $g = L_k^{-1} f \in \mathrm{Dom}(L_k)$ for any $f \in L^2([-1,1])$.

We next parameterize the eigenvalue $\lambda \in \mathbb{C}$ in the form

$$\lambda = -\nu(\nu+1). \tag{30}$$

In view of the parameterization (30), it is convenient to rewrite the second equation of system (25) as the associated Legendre equation

$$\frac{d}{dz}\left[(1-z^2)\frac{df}{dz}\right] - \frac{\sigma^2}{1-z^2} f + \nu(\nu+1) f = 0, \tag{31}$$

where ν is an arbitrary complex constant and

$$\sigma = (k^2 + ikR_e)^{1/2} \tag{32}$$

is a complex parameter such that $\mathrm{Re}(\sigma) \geq k \geq 1$ for any $R_e \geq 0$ and $k \in \mathbb{N}$. This means that the two linearly independent solutions of the associated Legendre Eq. (31) have the asymptotic behavior $(1-z^2)^{\sigma/2}$ and $(1-z^2)^{-\sigma/2}$ as $z \to \pm 1$. The second solution must be excluded because it is not in $L^2([-1,1])$ for any σ with $\mathrm{Re}(\sigma) \geq 1$. As is well-known from the reduction of the associated Legendre equation to the hypergeometric equation (see e.g., our previous paper[21]), a solution of (31) does not diverge as $z \to \pm 1$ if and only if it is a polynomial solution. The polynomial solutions exist if $\nu = \nu_n \equiv \sigma + n$, where $n \geq 0$ is integer. Therefore, the exact distribution of eigenvalues of the linearized problem (25) is given by

$$\lambda_n = -\nu_n(\nu_n+1), \tag{33}$$

where

$$\nu_n = (k^2 + ikR_e)^{1/2} + n, \quad n \geq 0. \tag{34}$$

The corresponding eigenfunction $f(z)$ is $P^{\sigma}_{n+\sigma}(z)$.

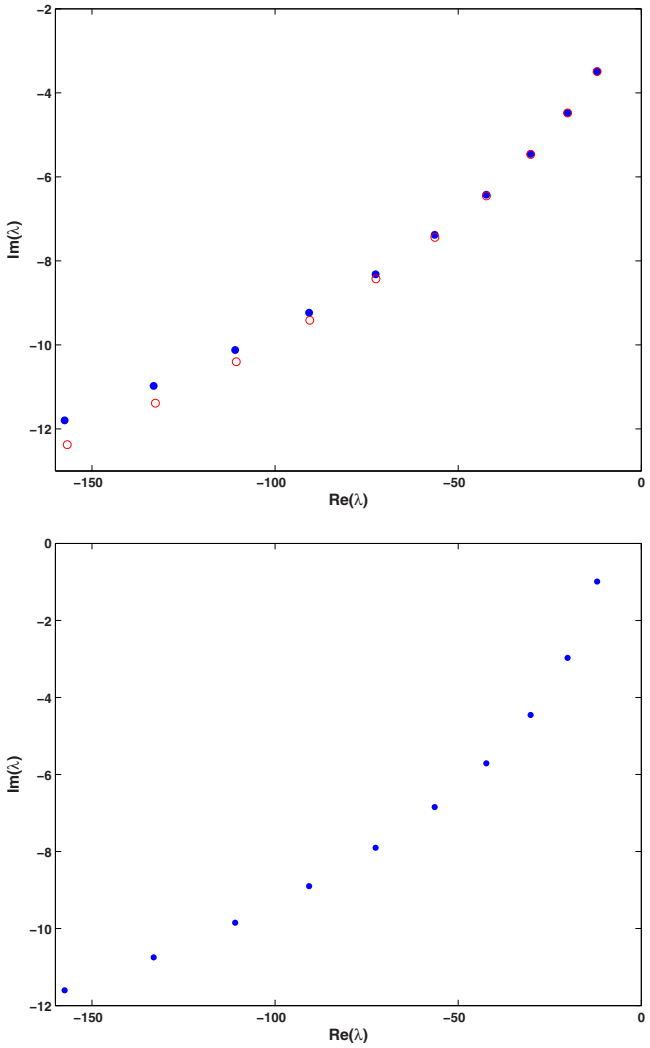

FIG. 1. (Color online) Approximation of the first ten eigenvalues numerically (dots) and analytically (open circles) for $z_0=0.999$, $k=3$, $R_e=1$, and either $\delta=0$ (top) or $\delta=10$ (bottom).

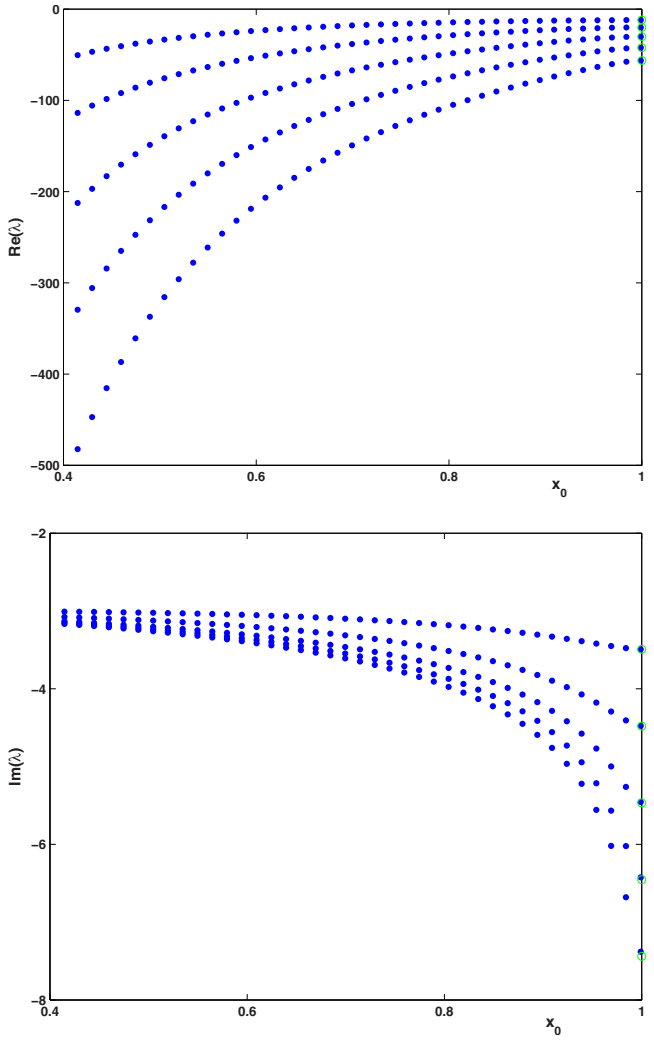

FIG. 2. (Color online) Approximation of the first five eigenvalues numerically (dots) and analytically (open circles) vs z_0 for $\delta=0$, $k=3$, and $R_e=1$.

B. The case of nonzero rotation

The full linearized problem (26) can be written as

$$L_k g = f, \quad L_k f = \lambda f + ik\left(\frac{R_e f}{1-z^2} + \delta g\right), \tag{35}$$

where we denote $\delta=R_e/R_0$. Inverting L_k as in the above, we obtain a closed eigenvalue problem

$$L_k f - ikM_k f = \lambda f, \tag{36}$$

where

$$M_k = \frac{R_e}{1-z^2} + \delta L_k^{-1}. \tag{37}$$

Since L_k is a symmetric operator on $L^2([-1,1])$, the operator M_k is also a symmetric operator, which implies that for each eigenvalue λ with the L^2-normalized eigenfunction $f \in \mathrm{Dom}(L_k)$, we have

$$\mathrm{Re}(\lambda) = (L_k f, f) < 0, \quad \mathrm{Im}(\lambda) = -k(M_k f, f). \tag{38}$$

The first relation in Eq. (38) confirms the asymptotic stability of the stationary exact solution (13) since $\mathrm{Re}(\lambda)<0$ for all eigenvalues for the linearized problem (35).

Although the corresponding eigenvalues are not available in closed analytical form, perturbation theory implies that all eigenvalues λ_n of the limiting problem with the eigenfunctions $P^{\sigma}_{n+\sigma}$ can be expanded into the perturbed series to obtain

$$\lambda_n(\delta) = -\nu_n(\nu_n+1) - ik\delta\frac{(L_k^{-1}P^{\sigma}_{n+\sigma}, P^{\sigma}_{n+\sigma})}{\|P^{\sigma}_{n+\sigma}\|^2} + \mathcal{O}(\delta^2), \quad \text{as} \quad \delta \to 0 \tag{39}$$

for an integer $n \geq 0$. In particular, since L_k^{-1} is self-adjoint, for each $n \geq 0$ we have

$$\mathrm{Re}[\lambda_n(\delta)] - \mathrm{Re}[\lambda_n(0)] = \mathcal{O}(\delta^2), \qquad \mathrm{Im}[\lambda_n(\delta)] - \mathrm{Im}[\lambda_n(0)] = \mathcal{O}(\delta), \quad \text{as} \quad \delta \to 0. \tag{40}$$

V. NUMERICAL APPROXIMATIONS OF EIGENVALUES

For the purpose of numerical approximations, system (35) is defined on the symmetric interval $[-z_0,z_0]$, where $z_0=\cos(\theta_0)$, which corresponds to the truncated annular domain

$$S_0=\{(\theta,\phi):\theta_0\le\theta\le\pi-\theta_0,\ 0\le\phi\le 2\pi\}, \tag{41}$$

where $0<\theta_0<\pi/2$. Without loss of generality, the spherical layer S_0 is truncated symmetrically at the two rings located in the northern and southern semispheres so that the stationary flow (13) is free of pole singularities in S_0. The analytical predictions of Sec. IV correspond to the limiting case $z_0\to 1$.

Following a computational method in our previous work,[21] we shall consider solutions of the linearized system (26) on $[-z_0,z_0]$ with boundary conditions

$$g(\pm z_0)=0,\quad g'(\pm z_0)=0. \tag{42}$$

Convergence of eigenvalues of the linearized problem on the truncated domain $[-z_0,z_0]$ subject to the boundary conditions (42) to eigenvalues of the same linearized problem on the full domain $[-1,1]$ subject to the boundary condition (28) follows from an analog of theorem 5.3 in Bailey *et al.*[25]

We look for the following power series solution of the spectral problem (35):

$$f(z)=\sum_{m\ge 0}a_m z^{2m}+\sum_{m\ge 0}b_m z^{2m+1}, \tag{43}$$

$$g(z)=\sum_{m\ge 0}c_m z^{2m}+\sum_{m\ge 0}d_m z^{2m+1}, \tag{44}$$

where the starting coefficients (a_0,b_0,c_0,d_0) are parameters.

Substituting (43) into the second equation of the linearized system (35), we find that (a_1,b_1) are defined by

$$a_1=\frac{[k^2-\nu(\nu+1)+ikR_e]a_0+ik\delta c_0}{2}, \tag{45}$$

$$b_1=\frac{[k^2+2-\nu(\nu+1)+ikR_e]b_0+ik\delta d_0}{6} \tag{46}$$

while the coefficients $\{a_m,b_m\}_{m\ge 2}$ are defined by the following recurrence relations:

$$a_{m+2}=\frac{[k^2-\nu(\nu+1)+8(m+1)^2+ikR_e]a_{m+1}+ik\delta c_{m+1}}{2(m+2)(2m+3)}+\frac{[\nu(\nu+1)-2m(2m+1)]a_m-ik\delta c_m}{2(m+2)(2m+3)} \tag{47}$$

and

$$b_{m+2}=\frac{[k^2-\nu(\nu+1)+2(2m+3)^2+ikR_e]b_{m+1}+ik\delta d_{m+1}}{2(m+2)(2m+5)}+\frac{[\nu(\nu+1)-2(2m+1)(m+1)]b_m-ik\delta d_m}{2(m+2)(2m+5)}. \tag{48}$$

We note that the initial Eqs. (45) and (46) follow from the recurrence Eqs. (47) and (48) for $m=-1$ if $a_{-1}=b_{-1}=0$.

Substituting Eq. (44) into the first equation of the linearized system (35), we find that the coefficients $\{c_m,d_m\}_{m\ge 2}$ are defined by the following recurrence relations:

$$c_{m+2}=\frac{[k^2+8(m+1)^2]c_{m+1}-2m(2m+1)c_m+a_{m+1}-a_m}{2(m+2)(2m+3)}, \tag{49}$$

$$d_{m+2}=\frac{[k^2+2(2m+3)^2]d_{m+1}-2(m+1)(2m+1)d_m+b_{m+1}-b_m}{2(m+2)(2m+5)}. \tag{50}$$

Similarly to the above, the initial equations for (c_1,d_1) follow from the recurrence Eqs. (49) and (50) for $m=-1$ if $a_{-1}=b_{-1}=c_{-1}=d_{-1}=0$ and they take the form

$$c_1=\frac{k^2c_0+a_0}{2},\quad d_1=\frac{(k^2+2)d_0+b_0}{6}. \tag{51}$$

The boundary conditions (42) lead to the following equations:

$$\sum_{m\ge 0}c_m z_0^{2m}=0,\quad \sum_{m\ge 0}d_m z_0^{2m+1}=0 \tag{52}$$

and

$$\sum_{m\ge 0}(2m)c_m z_0^{2m-1}=0,\quad \sum_{m\ge 0}(2m+1)d_m z_0^{2m}=0. \tag{53}$$

The boundary conditions (52) and (53) can be written as the homogeneous linear system

$$A(\nu)\vec{x}=0, \tag{54}$$

where $\vec{x}=[a_0,b_0,c_0,d_0]^T$ is the vector of initial data and $A(\nu)$ is a four-by-four matrix computed from the entries of boundary conditions (52) and (53). Correspondingly, the matrix $A(\nu)$ depends on $\nu\in\mathbb{C}$ as well as parameters $z_0\in(0,1)$, $R_e\in\mathbb{R}_+$, $\delta\in\mathbb{R}_+$, and $k\in\mathbb{N}$. If the power series are truncated at the M-term, the matrix $A(\nu)$ depends also on M. Eigenvalues $\lambda=-\nu(\nu+1)$ are equivalent to the roots of the determinant equation

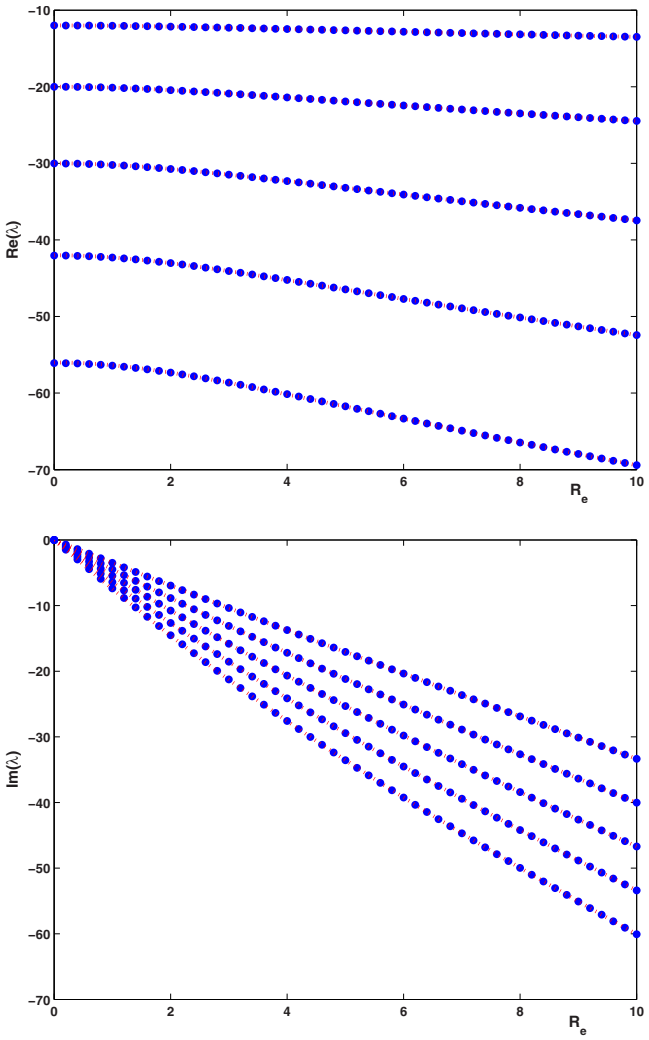

FIG. 3. (Color online) Approximation of the first five eigenvalues numerically (dots) and analytically (dotted line) vs R_e for $\delta=0$, $k=3$, and $z_0=0.999$.

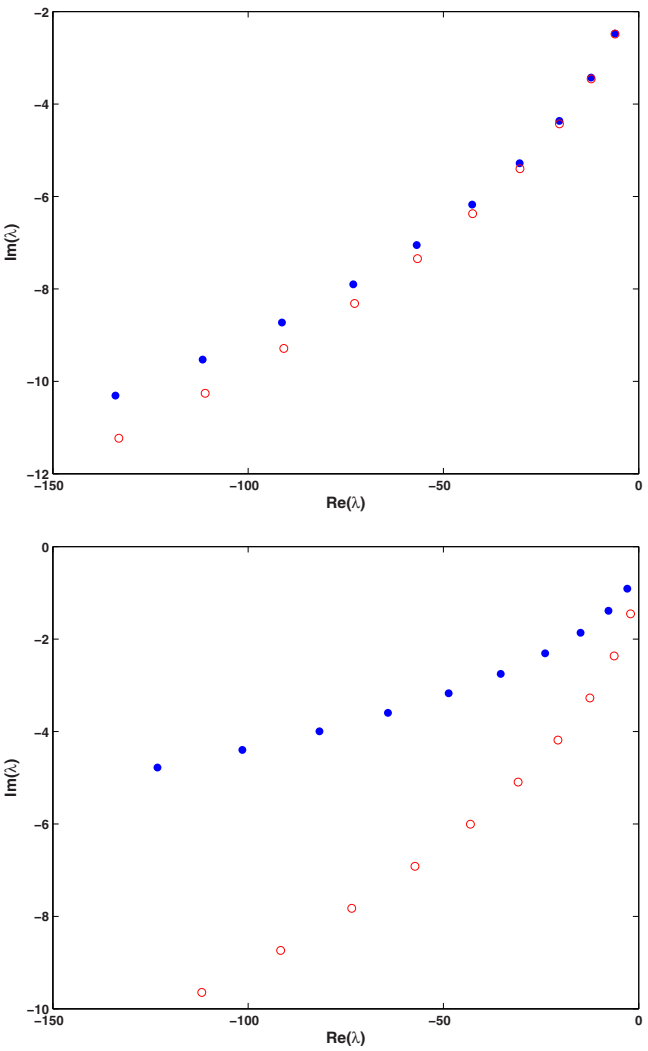

FIG. 4. (Color online) Approximation of the first ten eigenvalues numerically (dots) and analytically (open circles) for $z_0=0.99999$, $R_e=1$, $\delta=0$, and either $k=2$ (top) or $k=1$ (bottom).

$$F(\nu;z_0,R_e,\delta,k,M)=\det[A(\nu)]. \tag{55}$$

Figures 1 shows results of numerical computations for $z_0=0.999$, $R_e=1$, $k=3$, $M=200$, and either $\delta=0$ (top) or $\delta=10$ (bottom). The first ten eigenvalues $\lambda=-\nu(\nu+1)$ obtained from the roots of the function $F(\nu;z_0,R_e,\delta,k,M)$ are shown by dots on the complex plane. The theoretical approximation (34) is also shown by open circles on the top panel. We can see that the agreement is good for the first few eigenvalues but deviates for larger eigenvalues. We also observe that all eigenvalues are located in the left half-plane of λ, which indicates asymptotic stability of the stationary flow.

Figures 2 displays the real and imaginary parts of the first five roots of $F(\nu;z_0,R_e,\delta,k,M)$ versus z_0 together with the theoretical approximation (34) valid for $z_0=1$. Figures 3 shows the behavior of the first five roots and eigenvalues versus R_e for $z_0=0.999$.

The numerical approximations become even more accurate if the values of k are larger. However, for $k=1$ and $k=2$, the numerical approximation suffers from large round-off errors in the numerical algorithm. Figure 4 shows the first ten eigenvalues for $z_0=0.99999$, $R_e=1$, $\delta=0$, $M=1000$, and either $k=2$ (top) or $k=1$ (bottom). In spite of the proximity of z_0 to 1 and the large number of terms $M=1000$ in the power series, the agreement between the numerical and theoretical approximations is worse for $k=2$ and really bad for $k=1$.

Figure 5 shows the behavior of the real (top) and imaginary (bottom) parts of the first eigenvalue versus δ for $z_0=0.9999$, $R_e=1$, $k=5$, and $M=200$. The numerical approximations (dots) are superposed with the best power fit (dotted line). According to the theoretical prediction (40), the imaginary part of eigenvalues changes linearly in δ. However, the real part of eigenvalues is so small (it is supposed to change quadratically in δ) that the numerical approximation suffers from large round-off error. As a result, the best power fit does not allow us to recover the quadratic behavior of the real part of eigenvalues in δ.

VI. DISCUSSION

We have investigated the linearized stability of the latitude-dependent viscous flow (8) which represents stationary exact solution of the two-dimensional NS Eqs. (4)–(6) on a rotating spherical surface. The latter exact solution can be

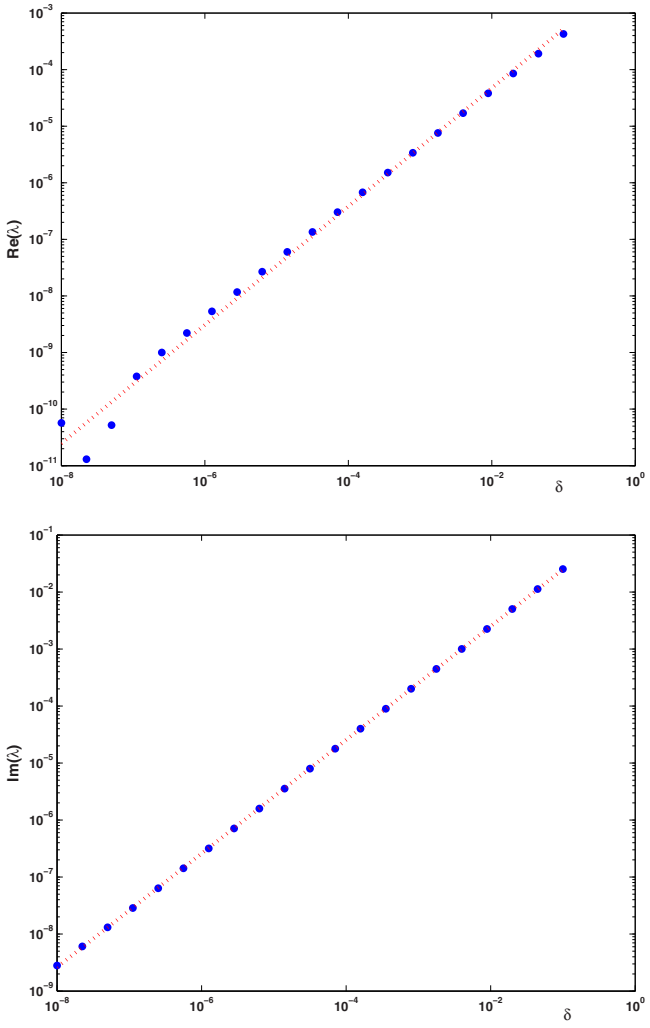

FIG. 5. (Color online) Behavior of the real (top) and imaginary (bottom) parts of the first eigenvalue vs δ from the numerical approximation (dots) and from the best power fit (dotted line) for $z_0=0.99999$, $R_e=5$, and $k=3$.

associated with a cyclonic rotation around the poles, i.e., the general west-to-east flows between the Ferrell and Polar cells. It has been proven analytically that the stationary flow (8) is asymptotically stable. When the spherical surface is truncated between two symmetrical rings near the poles, the asymptotic stability has been verified numerically by showing that the real parts of all isolated eigenvalues are negative for all Reynolds numbers. Additionally, the corresponding eigenvalues were derived in closed analytical form for the case of zero rotation and the asymptotic behavior of eigenvalues for a nonzero rotation has been obtained by means of perturbation theory.

From a practical standpoint, understanding of eigenvalue distribution can be used in meteorological applications, e.g., to estimate the dependence of the speed of small meanders of the west-to-east flows on the wave parameters k and n.

We have also found that the numerical approximations based on the power series expansions suffer from large round-off errors for small values of δ. One of our further goals is to improve the numerical scheme to recover a correct behavior of $\mathrm{Re}(\lambda)$ versus δ for this case. Another goal of the forthcoming studies is to develop further our present model to investigate atmospheric motions that are more physically relevant to oceanographic applications. To this end we aim to consider realistically large values of δ and to include the frictional effects (for example, due to small-scale turbulence) as well as heating.

For further studies, we intend to adopt the numerical approximations based on the Jacobi–Davidson "QZ" method.[18] Namely, we would like to recover first the case when the frictional effects and heating are ignored. Since the numerical method is based on calculating eigenvalues that are closest to a prespecified target value, this direction seems promising because, in the case of no friction and heating, the distribution of the eigenvalues (that can be obtained numerically by means of the present analysis) can serve as the required prespecified values of λ_n when $\delta \neq 0$ and the effects of friction and heating are included.

[1] E. N. Blinova, "A hydrodynamical theory of pressure and temperature waves and of centers of atmospheric action," C. R. (Dokl.) Acad. Sci. URSS **39**, 257 (1943).
[2] E. N. Blinova, "A method of solution of the nonlinear problem of atmospheric motions on a planetary scale," Dokl. Akad. Nauk SSSR (N.S.) **110**, 975 (1956).
[3] J. L. Lions, R. Teman, and S. Wang, "On the equations of the large-scale ocean," Nonlinearity **5**, 1007 (1992).
[4] J. L. Lions, R. Teman, and S. Wang, "New formulations of the primitive equations of atmosphere and applications," Nonlinearity **5**, 237 (1992).
[5] R. N. Ibragimov, "Shallow water theory and solutions of the free boundary problem on the atmospheric motion around the Earth," Phys. Scr. **61**, 391 (2000).
[6] D. Iftimie and G. Raugel, "Some results on the NS equations in thin three-dimensional domains," J. Differ. Equations **169**, 281 (2001).
[7] W. Weijer, F. Vivier, S. T. Gille, and H. Dijkstra, "Multiple oscillatory modes of the Argentine Basin. Part II: The spectral origin of basin modes," J. Phys. Oceanogr. **37**, 2869 (2007).
[8] C. P. Summerhayes and S. A. Thorpe, *Oceanography: An Illustrative Guide* (Wiley, New York, 1996).
[9] G. K. Bachelor, *An Introduction to Fluid Dynamics* (Cambridge University Press, Cambridge, 1967).
[10] E. Herrmann, "The motions of the atmosphere and especially its waves," Bull. Am. Math. Soc. **2**, 285 (1896).
[11] O. M. Belotserkovskii, I. V. Mingalev, and O. V. Mingalev, "Formation of large-scale vortices in shear flows of the lower atmosphere of the Earth in the region of tropical latitudes," Cosmic Res. **47**, 466 (2009).
[12] C. Cenedese and P. F. Linden, "Cyclone and anticyclone formation in a rotating stratified fluid over a sloping bottom," J. Fluid Mech. **381**, 199 (1999).
[13] J. R. Toggweiler and J. L. Russel, "Ocean circulation on a warming climate," Nature (London) **451**, 286 (2008).
[14] R. F. Anderson, S. Ali, L. L. Brandtmiller, S. H. H. Nielsen, and M. Q. Fleisher, "Wind-driven upwelling in the Southern Ocean and the deglacial rise in atmospheric CO_2 ," Science **323**, 1443 (2009).
[15] D. T. Shindell and G. A. Schmidt, "Southern hemisphere climate response to ozone changes and greenhouse gas increases," Geophys. Res. Lett. **31**, L18209, doi:10.1029/2004GL020724 (2004).
[16] R. Temam and M. Ziane, "NS equations in thin spherical domains," Contemp. Math. **209**, 281 (1997).
[17] G. Ben-Yu, "Spectral method for vorticity equations on spherical surface," Math. Comput. **64**, 1067 (1995).
[18] G. L. G. Sleijpen and H. A. Van der Vorst, "A Jacobi–Davidson iteration method for linear eigenvalue problems," SIAM J. Matrix Anal. Appl. **17**, 410 (1996).
[19] D. Williamson, J. B. Drake, and J. J. Hack, "A standard test for numerical approximation to the shallow water equations in spherical geometry," J. Comput. Phys. **102**, 211 (1992).

[20]T. G. Callaghan and L. K. Forbes, "Computing large-amplitude progressive Rossby waves on a sphere," J. Comput. Phys. **217**, 845 (2006).
[21]R. N. Ibragimov and D. E. Pelinovsky, "Incompressible viscous fluid flows in a thin spherical shell," J. Math. Fluid Mech. **11**, 60 (2009).
[22]P. N. Swarztrauber, "Shallow water flow on the sphere," Mon. Weather Rev. **132**, 3010 (2004).
[23]H. Lamb, *Hydrodynamics*, 5th ed. (Cambridge University Press, Cambridge, 1924).
[24]E. Zeidler, *Applied Functional Analysis: Applications to Mathematical Physics* (Springer-Verlag, New York, 1995).
[25]P. B. Bailey, W. N. Everitt, J. Weidmann, and A. Zettl, "Regular approximations of singular Sturm–Liouville problems," Results Math. **23**, 3 (1993).